JOURNAL OF MATERIALS SCIENCE 25 (1990) 1381–1391

Characteristics of rapidly solidified Al–Si–X preforms produced by the Osprey process

J. L. ESTRADA, J. DUSZCZYK
Laboratory for Materials Science, Faculty of Chemical Technology and Materials Science, Delft University of Technology, Rotterdamseweg 137, 2628 AL Delft, The Netherlands

This paper describes some characteristics of an Al–20Si–X aluminium alloy, processed by the Osprey route, in terms of total oxygen content, porosity distribution and microstructure. A theoretical analysis of the solidification of the material, after a semi-liquid/semi-solid spray of atomized droplets–particles impacts the deposit, is presented. A heat flow calculation was conducted applying the forced convection method at quasi-steady conditions. Based on the calculation of the heat transfer coefficient the cooling rate was estimated within the range $\sim 10^2$ to 10^4 K sec^{-1}. Stroehlein OSA–MAT measurements showed that the total content of oxygen of the Osprey preform was 3.5 and 7 times lower than the corresponding values for argon (nitrogen) and air atomized Al–20Si–X powders, respectively. Light microscopic examination of the deposited material revealed a homogeneous microstructure with a porosity level as low as 1.3%. Microstructural features indicated that the Osprey process provided rapidly solidified material with an average cooling rate of 10^3 to 10^4 K sec^{-1}. This cooling range proves that the theoretical estimation presented in this work is sufficiently accurate.

1. Introduction

Considerable success has been achieved in the last decade in the development of advances aluminium alloys which offer enhanced properties compared to conventional, wrought products. Most of these developments have centred on P/M (powder metallurgy) and other rapid solidification technologies which permit new alloy compositions to be processed without the limitation imposed by conventional casting [1, 2]. The principal advantages to be gained arise from macro-segregation elimination yielding mechanical property improvements, and from the near-net shaping capability. Another advantage is that the fine resulting grain size produces excellent workability and also grain-size strengthening at high temperatures. However, despite the attractions of these rapid solidification techniques, the current application of such new alloys is limited, mainly because of multistep processes which involve higher costs than alternate production routes such as casting [3, 4]. This limitation is particularly important in the automotive industry where products with improved properties can usually only be sold in combination with a low manufacturing cost.

Consequently, a process which can offer both superior properties and low processing costs is particularly attractive. It is believed that among various relatively well developed new solidification techniques the Osprey process has the ability to fulfil these requirements [5]. The Osprey process, pioneered by Singer [6, 7] and later developed commercially by Leatham, Brooks and Coombs [8, 9], is a rapid solidification process capable of producing near-net shaped products or coated articles in a single, integrated operation. The process [10] comprises the steps of providing a stream of molten metal, converting the metal stream into a spray of molten droplets by gas-atomization and directing the droplets at a collecting surface where they re-coalesce to form a high density shaped spray-deposit (preform). The resulting deposit can either be used in the as-deposited form (either bonded to or removed from the collector), or it can be further processed, again either bonded to or separate from the collector, by conventional working operations. The rapid solidification results in deposits which are characterized immediately after deposition by a fine, uniform grain size without macro-segregation, irrespective of the thickness of the deposit [10].

Figure 1 shows a schematic diagram of the arrangement for aluminium preform production with the option to produce particulate composite materials. A section of an aluminium alloy preform, produced in 35 sec with a gas to metal ratio of 3.5 m^3 kg^{-1}, is shown in Fig. 2 [11]. To produce such a preform a stream of molten aluminium is dispensed from a furnace, directly into a gas-atomizing device at metal flow-rates which are typically in the range 5 to 25 kg min^{-1}. The metal stream is then impacted by high velocity jets of atomizing gas (normally nitrogen) which serves several essential functions, namely:

1. To comminute the stream into a spray of fine droplets; for aluminium alloys the mean droplet size is typically 25 to 40 μm.

2. To shape and rapidly move the spray; in this way a high yield of metal is deposited and the desired preform shape is obtained. Deposition yields are typically in the range 70 to 90%, depending mainly on the size and shape of the preform being deposited.

3. To protect the atomized droplets from oxidation;

0022–2461/90 $03.00 + .12

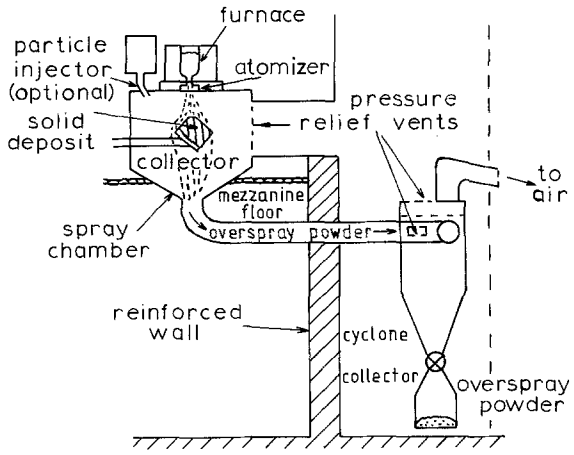

Figure 1 Schematic representation of aluminium preform production (including metal matrix composites: MMCs).

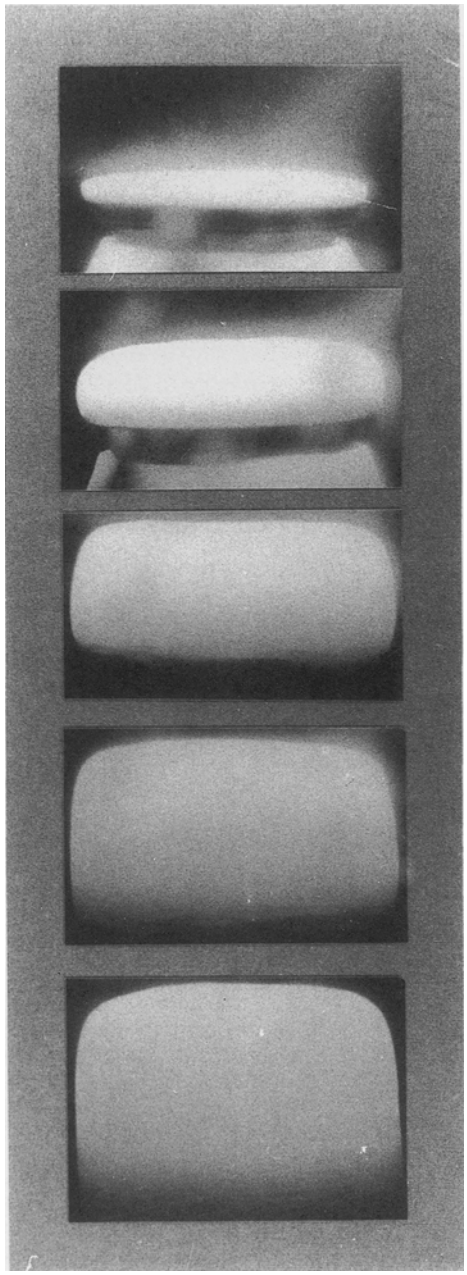

Figure 2 Section of an aluminium alloy preform – spraying time 35 sec (Osprey Metals Ltd).

the nitrogen used for atomization is evaporated from a standard, high purity, liquid source and because the droplet flight time is only a few milliseconds, no significant oxidation of the droplets occurs.

4. To transfer kinetic energy from the high velocity gas to the atomized droplets; this assists in the formation of high density preforms.

5. To rapidly extract a controlled amount of heat from the droplets, both in flight and on deposition; this is essential to the production of rapidly solidified preforms, irrespective of section thickness.

The widespread interest and development of spray-deposition (the Osprey process) can be ascribed to several flexibly interrelated factors whose characteristic is increasingly demanded when specifying processes or materials to meet the demands of new products. Although the Osprey process for aluminium alloys can be described as incorporating the advantages of powder metallurgy without the disadvantages of degassing and consolidation, it is more useful to mention some options that become available when this route is followed [12, 13]:

(a) The rapid formation of a range of semi-finished products such as tubes, billets or strip directly from the melt. Coated products can also be manufactured.

(b) The processing of difficult to work conventional alloys and novel alloy compositions as a direct consequence of rapid solidification.

(c) The creation of composite products which can contain over 20 volume % dispersoid by injection of particulate into the atomized stream of molten alloy (Fig. 1).

(d) A range of secondary processing routes can be considered without prolonged soaking times and/or large deformation ratios being necessary as a result of fine grain size, segregation-free, non-dendritic microstuctures.

It has been described in the literature that the microstructure of spray deposited materials varies depending upon different processing conditions. Apelian, Kear and Schadler [14] emphasize that among many factors which contribute to the final microstructure of the Osprey material, the most important are droplet–particle velocities, size distribution, temperature profiles and droplet–substrate interactions. The latter is crucial since it affects the cooling rate, microporosity and hence the microstructure. In turn the cooling rate has an important effect on the development of the microstructure before, during and after solidification [15].

Although the Osprey process is assumed to be performed with a cooling rate of 10^3 to 10^7 K sec^{-1} [9, 16, 17], there are still not enough experimental and theoretical data proving that an actual cooling rate of spray-deposited material is within the rapid solidification range. Therefore, it was necessary to undertake a theoretical and experimental study on the solidification characteristics, cooling rate and microstructure of an Osprey preform.

2. Experimental procedure

The spray-deposited preform studied was produced by Osprey Metals using nitrogen for atomization. The

TABLE I Nominal composition of the Material studied, wt %

Si	Cu	Mg	Fe	Al
20.0	3.1	1.3	0.3	bal.

nominal composition of the material investigated is given in Table I.

A theoretical analysis of the solidification of the material, after a spray of atomized droplets (particles) in semi-liquid/semi-solid state impacts the deposit, is presented. A heat flow calculation was conducted applying the forced convection method at quasi-steady conditions. Based on the calculation of the heat transfer coefficient the cooling rate was estimated.

The total content of oxygen was measured by means of the Stroehlein OSA-MAT method. Porosity measurements, of small prisms taken from a cross section of the preform along the plane of spraying, were provided by autopycnometry in helium (with evaporation of moisture at 120° C for 5 minutes).

Description of the microstructure was provided by optical microscopic examination of samples prepared by a standard metallographic technique, followed by etching with a 1% solution of nitric acid in Wilcox and Keller's reagent.

3. Results and discussion

3.1. On-deposition solidification

As already described [9, 12, 18], upon the instant of impingement (deposition) a range of droplet sizes can be at different temperatures and states of solidification. For a given alloy and atomizing gas the cooling rate in flight is mainly determined by the size of an individual particle since the size strongly governs the amount of heat that must be dissipated from the droplets in flight prior to impact. An extended discussion on the cooling rate and solidification mode of atomized Al–20Si–X alloys, in terms of atomizing gas, gas velocity and particle diameter, was presented in a previous publication [19]. Under optimum conditions, the coarse particles are deposited in the fully molten state and the fine particles will be deposited fully solidified at a temperature close to that of the atomizing gas. From experimental observations, it is believed that the majority of particles of an intermediate size will be deposited in the semi-solid/semi-liquid condition, or in an undercooled state (Fig. 3) [11]. This is also reported by Lavernia *et al.* [15] whose experimental results suggest that definite proportions of liquid and solid phases are required in the spray at the moment of impact for the attainment of sound deposits (the amount of liquid phase in the spray should be between 15 and 30%).

It is essential that the surface on to which the particles are deposited is not at too low a temperature as this leads to each individual particle retaining its own identity and characteristic microstructure after deposition [20]. Conversely, according to Leatham and Ogilvy [11, 12], the surface on to which the particles are deposited must not be at too high a temperature as a thick layer of molten alloy can build up on the surface of the preform and subsequently be ejected from the surface by the high velocity gas and/or motion of the collector. Needless to say the presence of such a fully liquid layer can lead to problems with the process since splashing can become excessive [21]. Ideally, the conditions of deposition are controlled in such a manner that a layer of semi-solid/semi-liquid metal of controlled thickness is maintained at the surface of the preform throughout the deposition operation. This is supported by the results obtained by G. Miravete *et al.* [22] which indicate that a small fraction of liquid mixed with solid exists at the top of the growing preform during deposition.

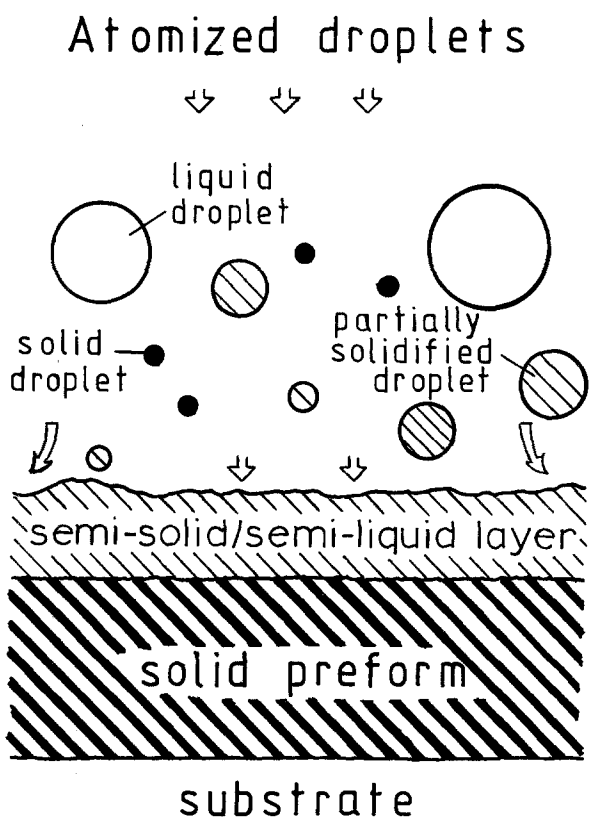

Figure 3 Schematic representation of the deposition stage of the Osprey Process.

It has been pointed out [12] that the particles in which dendritic solidification has occurred during flight are impacted at high velocity on to the surface of the preform resulting in dendrite fragmentation. The fine presolidified particles and the coarse (or undercooled) fully molten particles add to the solid and liquid content of the surface of the preform. Thus, the preform surface consists of a mixture of dendrite fragments, pre-solidified particles and liquid metal. The fine, pre-solidified particles and the dendrite fragments appear to re-melt in the liquid metal, aided partly by the release of latent heat.

The final microstructure of spray deposition will be determined both by the solidification prior to and after the impingement of the atomized particles on to the deposit surface. The latter is of particular interest for this study.

3.1.1. Heat transfer considerations and cooling rate

Heat extraction from the semi-solid/semi-liquid layer is assumed to be performed by conduction of heat to the substrate and extraction of heat by the fast moving

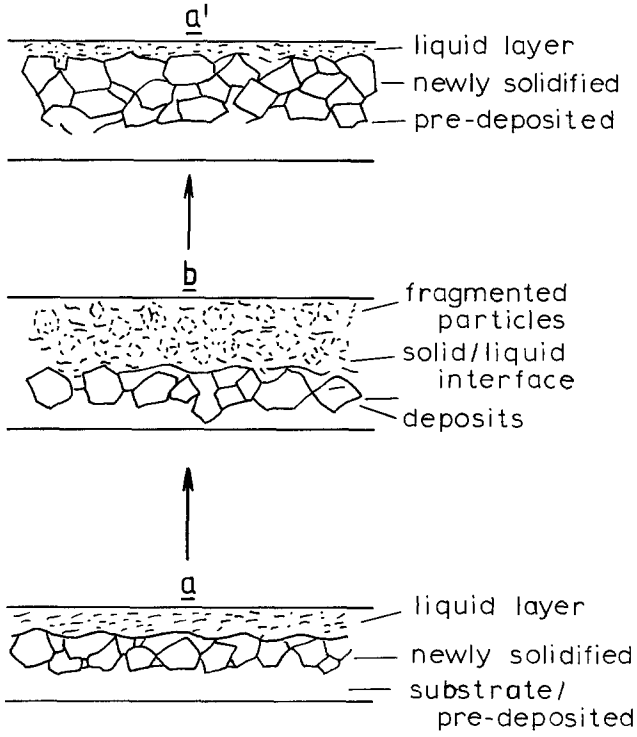

Figure 4 Schematic illustration of the on-deposition solidification.

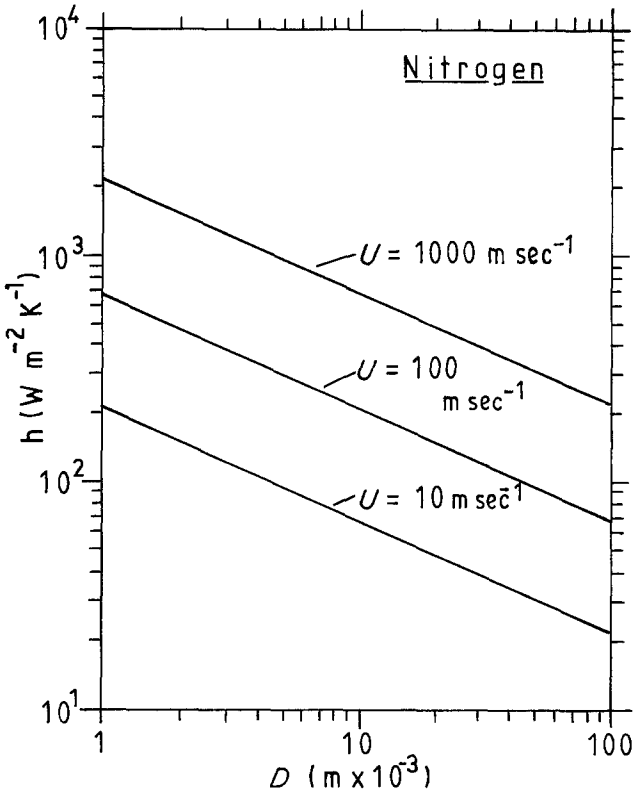

Figure 5 Gas–preform interfacial heat transfer coefficient as a function of the preform diameter at different gas (nitrogen) velocities.

atomizing gas. The conduction of heat to the substrate could be dominant at the initial transient stage of deposition. While the particles are deposited on a quite cold substrate, the degree of interface contact plays an important role. But in this particular case of spray deposition, as the thickness of the deposit increases, the cooling of the deposit has to rely mainly on heat transfer to the surroundings by forced convection of the relatively cold atomizing gas flowing over the deposit surface.

Apart from the initial and final transient stages of the deposition process, a constant supply of droplets to the deposit, a constant heat transfer from the layer to the flowing gas and hence a constant cooling rate during the process are assumed. Figure 4 illustrates schematically the deposition and solidification mechanism.

The heat transfer is considered to take place in a quasi-steady state. Since the states a and a' are common except for the increment of the deposit thickness, the complexity in dealing with the process from a to b and b to a' is therefore avoided. Another assumption made in this study is that the internal heat flow is practically isothermal. To evaluate the heat extraction from the film by the atomizing gas, the approach of the convection heat transfer, particularly dealing with laminar flow, is applied [23–25]. The effectiveness of this heat extraction is characterized by a heat transfer coefficient h.

In the case of convection from a flat plate over which a fluid is flowing, the heat transfer coefficient (h) is presented by [23]:

$$h = (k_g/D)\mathrm{Nu} \quad (1)$$

where Nu is given by

$$\mathrm{Nu} = 0.332\mathrm{Re}^{1/2}\,\mathrm{Pr}^{1/3} \quad (2)$$

Nu, Re and Pr are dimensionless groups called Nusselt number; Reynolds number and Prandtl number, respectively. They are expressed as:

$$\begin{aligned} \mathrm{Nu} &= hD/k_g \\ \mathrm{Re} &= (U\varrho_g/\mu_g)D \\ \mathrm{Pr} &= c_g\mu_g/k_g \end{aligned} \quad (3)$$

where h = heat transfer coefficient ($\mathrm{Wm^{-2}\,K^{-1}}$), U = gas velocity ($\mathrm{msec^{-1}}$), D = diameter of a preform (m), ϱ_g = gas density ($\mathrm{kgm^{-3}}$), c_g = heat capacity of the gas ($\mathrm{Jm^{-3}\,K^{-1}}$), k_g = thermal conductivity of the gas ($\mathrm{Wm^{-1}\,K^{-1}}$), μ_g = dynamic viscosity of the gas ($\mathrm{Nsm^{-2}}$).

The value of Pr is about unity (within a factor of perhaps two or three) for all gases under normal conditions [24]. Therefore a combination of Equations 1, 2 and 3, gives

$$h = 0.332\,k_g(\varrho_g/\mu_g)^{1/2}\,(U/D)^{1/2} \quad (4)$$

where all the thermophysical properties refer to the gas. The results of the calculation of the heat transfer coefficient (h), for nitrogen, by means of Equation 4, are given in Fig. 5. The thermophysical data of nitrogen gas, given in Table II, are taken from [26].

TABLE II Thermophysical data of nitrogen gas [26]

Property	Symbol	Units	Value
Thermal conductivity	k_g	$\mathrm{Wm^{-1}K^{-1}}$	3.33×10^{-2}
Density	ϱ_g	$\mathrm{kgm^{-3}}$	0.853
Dynamic viscosity	μ_g	$\mathrm{Nsm^{-2}}$	21.98×10^{-6}

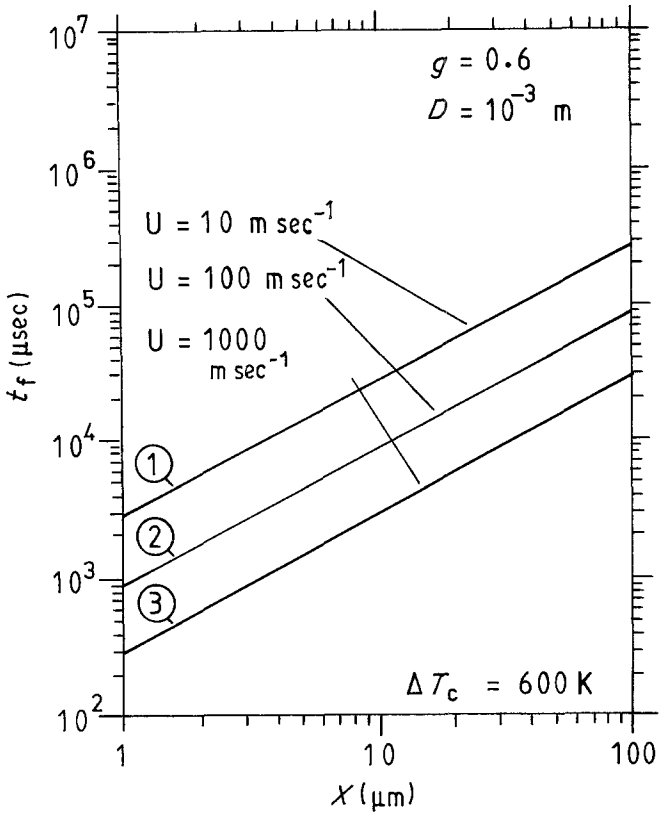

Figure 6 Local solidification time as a function of the solidifying film thickness for atomization in a stream of nitrogen (D = 1 mm).

It is apparent, from Equation 4, that the heat transfer coefficient depends on the atomizing gas, gas velocity and preform diameter. It is implied by the laminar flow theory that there is no lateral flow of the deposited semi-solid/semi-liquid layer (this is a unique feature of the spray deposition process distinguishing it from conventional casting).

The condition for Newtonian cooling during deposition is expressed as

$$h \ll k_m/X_m \tag{5}$$

where X_m is the thickness of the film and k_m is the thermal conductivity of the film material.

In the case of Newtonian cooling, the local solidification time, for a given heat transfer coefficient h, can be estimated by

$$t_f = \Delta H/h\Delta T_c A \tag{6}$$

where h is given by Equation 4, A is the surface area of the film, ΔH is the total heat that has to be removed and ΔT_c is expressed by

$$\Delta T_c = T - T_g \tag{7}$$

where T is the temperature of the film material and T_g is the temperature of the atomizing gas.

ΔH is given by

$$\Delta H = V(c_L \Delta T_s + \Delta H_f) \tag{8}$$

where V = volume of the solidified film material (m^3), c_L = specific heat of the liquid (Jm^{-3} K^{-1}), ΔH_f = latent heat of fusion (Jm^{-3}), and $\Delta T_s = T - T_f$ if the droplets (particles) are deposited at T, and the solidification temperature is T_f.

Suppose the film thickness is X, the area of the film A, and the fraction of solidified material g, then

$$\Delta H = AX(c_L \Delta T_s + \Delta H_f)(1 - g) \tag{9}$$

Substituting Equation 9 into Equation 6 gives

$$t_f = X(1 - g)(c_L \Delta T_s + \Delta H_f)/h\Delta T_c \tag{10}$$

From the preceding discussion it can be concluded that ΔT_s is a very uncertain factor that can vary from positive through zero to negative depending on the state of undercooling and solidification of the arriving droplets. Because of the relatively small effect of ΔT_s, the value of ΔT_s is taken to be zero and then Equation 10 becomes

$$t_f = X(1 - g)\Delta H_f/h\Delta T_c \tag{11}$$

The results of the calculation of the local solidification time, by means of Equation 11, for film thicknesses of 1 μm, 10 μm and 100 μm and a solid fraction of 0.6, at different velocities of the gas, for preform diameters of 1, 10 and 100 mm are shown in Figs 6, 7 and 8, respectively. This local solidification time is the time required for the solidification of the film to be completed. Figure 9 shows the overlapping of the results presented in Figs 6, 7, 8 and 9.

The thermophysical data of the aluminium preform, given in Table III, are taken from [27]. The fraction of solid phase, g, is assumed at the initial transient stage of the solidifying film. One can emphasize that g is dependent on the deposition rate. Figure 10 shows the local solidification time as a function of the fraction of solid phase of the preform layer (D =

TABLE III Thermophysical values for the aluminium preform [27]

Property	Symbol	Units	Value
Specific heat	c_L	Jm^{-3} K^{-1}	2.4 × 10^6
Latent heat of fusion	ΔH_f	Jm^{-3}	9.4 × 10^8

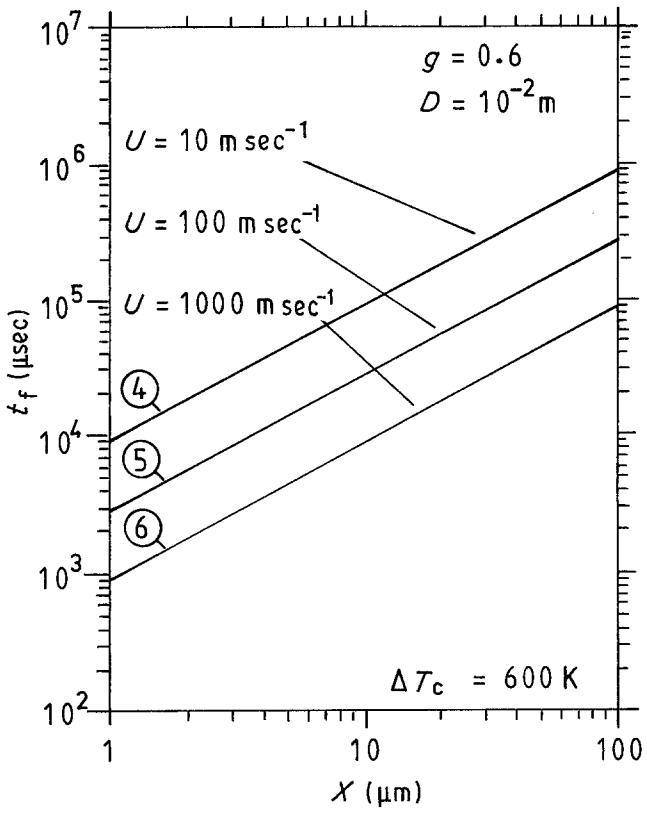

Figure 7 Local solidification time as a function of the solidifying film thickness for atomization in a stream of nitrogen (D = 10 mm).

150 mm, see Fig. 12) for a given film thickness at different velocities of the gas.

Rapidly solidified microstructures depend strongly on the cooling rate of the liquid phase [28]. For very high cooling rates (10^7 K sec^{-1} and higher) a featureless microstructure can be obtained. In most cases of industrial rapid solidification processes the microstructure is of the cellular/dendritic type with different scales as a result of varying cooling rates. These cooling rates are connected with the local solidification time.

The cooling rate has been estimated with the formula

$$e = h\Delta T_c / X c_L \qquad (12)$$

where e denotes the cooling rate in the period from the impingement of droplets/particles on to the deposit to the beginning of the solidification of a particular film, or, say, to the arrival of the next group of droplets/particles. The results of the calculation of the cooling rate, by means of Equation 12, as a function of the cooling film thickness at different gas velocities, are shown in Fig. 11. From these results the cooling rate

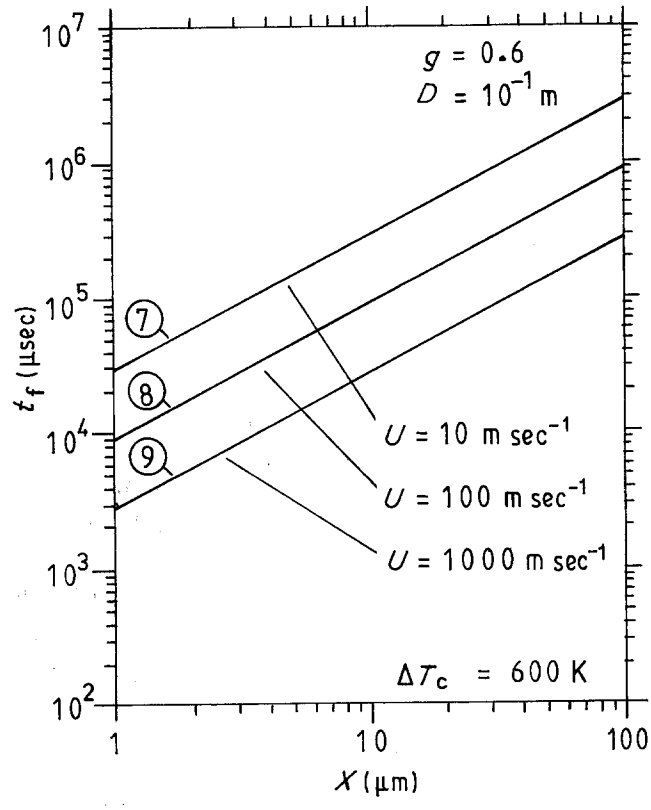

Figure 8 Local solidification time as a function of the solidifying film thickness for atomization in a stream of nitrogen (D = 100 mm).

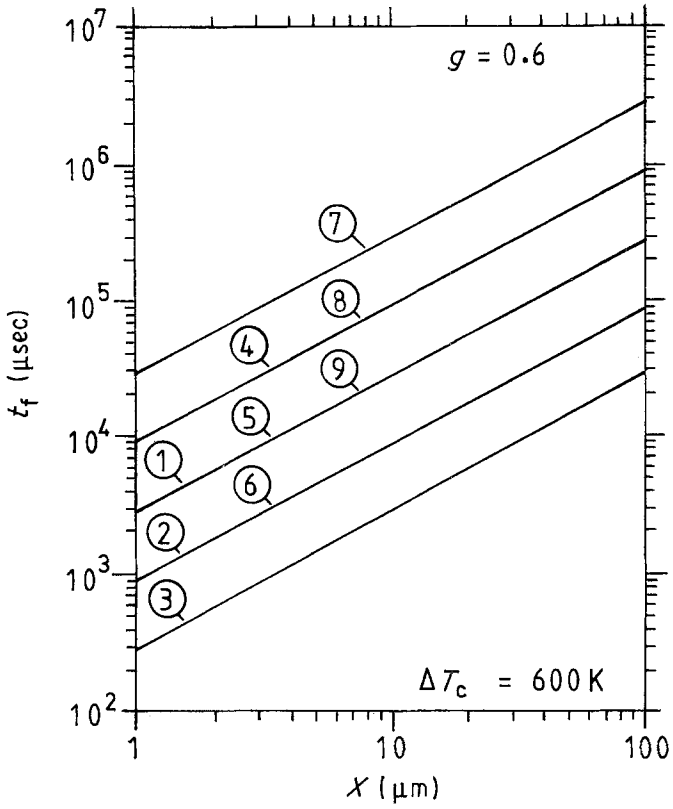

Figure 9 Local solidification time as a function of the solidifying film thickness for atomization in a stream of nitrogen for different preform diameters at different gas velocities (overlapping of Figs 6, 7 and 8).

was estimated in the range of $\sim 10^2$ to 10^4 K sec^{-1}. This range is in a good agreement with other rapid solidification techniques as, for instance, the production of metal powders by gas atomization [19, 29]. The results imply that the rapidly solidified structure can be obtained by spray deposition and that the Osprey preform process is a rapid solidification process.

3.2. Osprey preform

Figure 12 shows an Osprey preform, produced with a gas to metal ratio of 3.5 m^3 kg^{-1} [11], as well as the internal surface taken from a cross-section of the deposit. It is recognized that, with the exception of the side effects, the preform is built up from very thin and parallel distributed layers, perpendicular to the spraying direction, without cracks or shrinkages and without rejection of liquid from the semi-solid/semi-liquid metal surface of the preform. This is a clear indication that the deposition proceeds uniformly, layer by layer, without any influence of R (Fig. 12) and that the solidification mode is in a good agreement with the model assumed by Leatham and Ogilvy [11, 12].

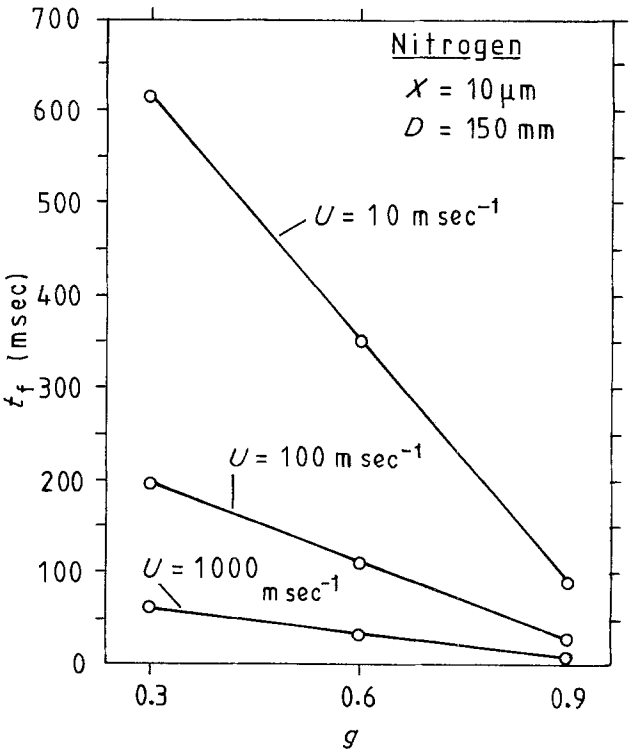

Figure 10 Local solidification time as a function of the fraction of solid phase of the preform layer for atomization in a stream of nitrogen at different gas velocities (D = 150 mm, see Fig. 12).

3.3. Microstructure

Porosity measurements obtained from one of the spray-deposited preforms are given in Fig. 13. These results were provided by autopycnometry in helium (with evaporation of moisture at 120° C for 5 minutes) of prisms taken from a cross-section of the preform along the plane of the spraying direction. The porosity was distributed relatively uniformly and varied from a minimum of 0.9% to a maximum of 1.6% with the average value being 1.3%; the size of the pores was typically in the range 5 to 40 μm.

The microstructure of a spray-deposited preform is homogeneous and free from macro-segregation (Fig. 14). It exhibited fine, uniform precipitation of silicon particles with an average size of 4 μm and a maximum size of 7 μm. It must be emphasized that this homogeneity is one of the most important characteristics of spray-deposited materials.

Light microscopic examination indicated that during the whole deposition period similar conditions in terms of heat extraction and deposition rate exist, providing a final uniform microstructure (Fig. 14). Another very important factor of spray-deposited

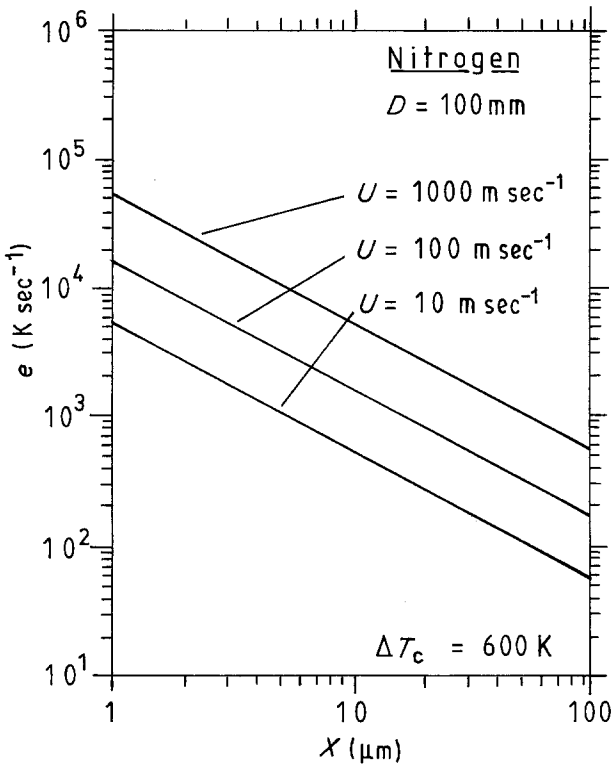

Figure 11 Cooling rate as a function of the cooling film thickness for atomization in a stream of nitrogen at different gas velocities.

materials concerns the absence of oxide film formation during atomization and deposition.

3.4. Relationship between silicon particle size and cooling rate

The relationship between solidification rate and dendrite cell size cannot be applied for determining the cooling rate of a spray-deposited material because of the lack of a "cast" cellular microstructure due to the fact that the mechanical action of splatting breaks off the dendrites of the semi-liquid/semi-solid particles at the point of deposition.

From the relationship between silicon particle size and cooling rate proposed in our previous works [5, 19, 31] it can be deduced that the mean cooling rates to form 4 to 7 μm silicon precipitates are in the range 10^3 to 10^4 K sec^{-1}. This cooling range proves that the theoretical estimation presented in this work is sufficiently accurate.

TABLE IV Oxygen contents of rapidly solidified aluminium materials [19]

Material		Atomization gas	Oxygen content wt %
J1	Al–20Si–3Cu–1Mg (powder)	air	0.203
J2	Al–20Si–3Cu–1Mg–5Fe (powder)	air	0.200
J3	Al–20S1–3Cu–1Mg–7.5Ni (powder)	air	0.220
K1	Al–20Si–5Fe–2Ni (powder)	air	0.213
K2	Al–20Si–5Fe–2Ni (powder)	argon	0.106
OS1	Al–20Si–3Cu–1Mg (overspray powder)	nitrogen	0.110
OS2	Al–20Si–3Cu–1Mg (preform)	nitrogen	0.030

3.5. Oxygen content

The content of oxygen, of the material investigated, was measured using the Stroehlein OSA-MAT. The

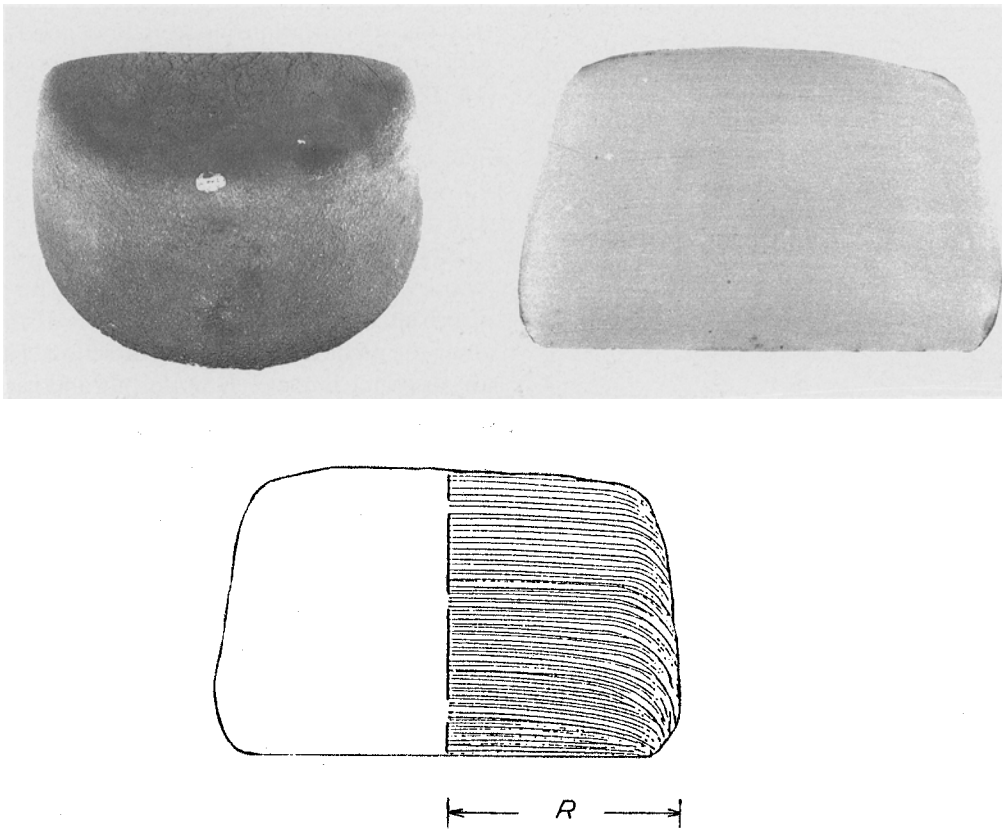

Figure 12 Osprey preform.

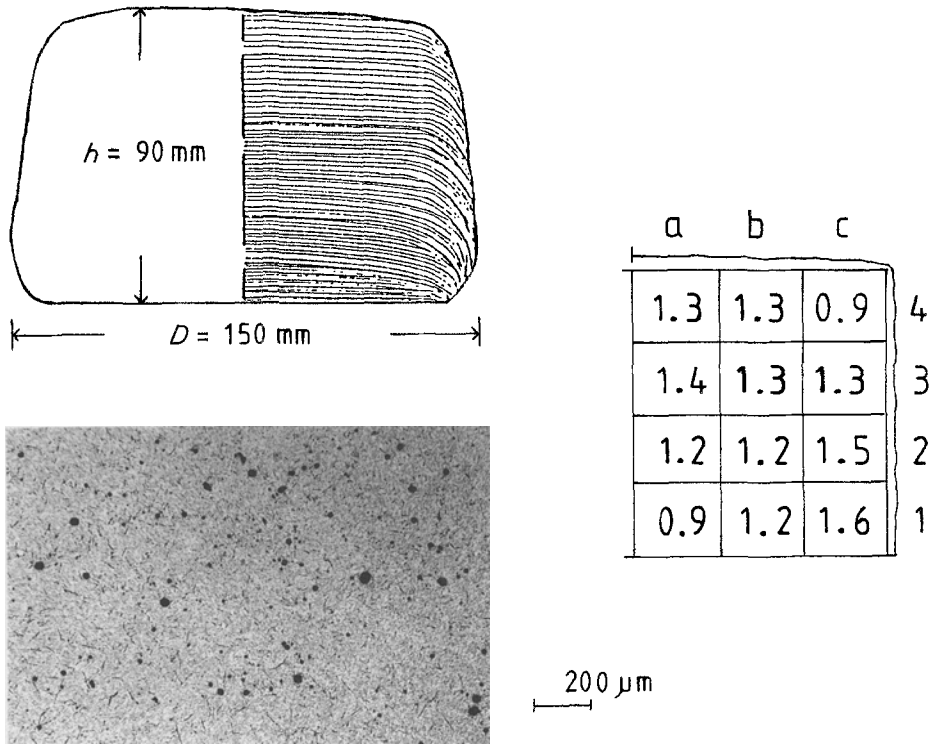

Figure 13 Porosity distribution of an Osprey preform as-sprayed.

principle of the method has already been described in detail [19].

Figure 15 presents the oxygen spectrum corresponding to the spray-deposited preform OS2:Al–20Si–3Cu–1Mg. The upper curve represents the second derivative curve of this oxygen spectrum. The X-axis of the lower curve gives the time of heating, whereas the Y-axis gives the relative speed of reduction of oxygen in per cent. The oxygen content is determined by the integral below the envelope curve.

The total oxygen content of the nitrogen atomized Osprey preform OS2:Al–20Si–3Cu–1Mg, namely 0.030 wt %, was compared with the total oxygen contents of the air atomized (for the powders J1, J2, J3, and K1) and the argon or nitrogen atomized (for the powders K2 or OS1) Al–20Si–X aluminium powders, previously obtained [19], whose corresponding values are gathered in Table IV. The values reported are averages from different samples.

It is apparent, from the results presented in Table IV, that the total oxygen contents of (i) the argon or nitrogen atomized powders (0.106 to 0.110 wt %) and (ii) the air atomized powders (average value 0.209 wt %) are 3.5 and 7 times higher, respectively, than 0.030 wt % corresponding to the total oxygen content of the nitrogen atomized Al–20Si–X Osprey preform OS2. This low oxygen content is one of the advantages that the Osprey process offers to minimize the problems associated with the oxide contamination of rapidly quenched powders that form difficult-to-reduce oxides [15]. The presence of a high volume fraction of oxides, particularly in stringer form in the worked alloys, has been shown to be highly detrimental to fracture toughness properties, fatigue crack growth

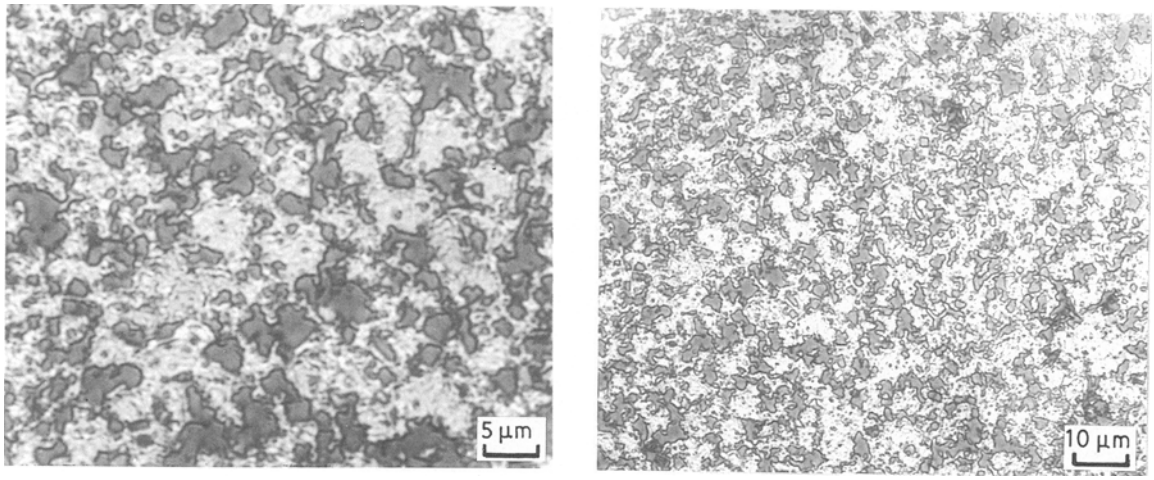

Figure 14 Microstructure of a spray-deposited preform.

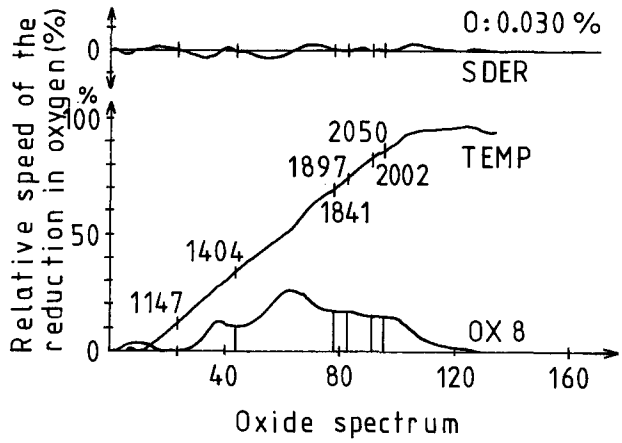

Figure 15 Oxide spectrum and second derivative of the oxide spectrum. Osprey preform as-sprayed OS2: Al–20Si–3Cu–1Mg.

rates and resistance to the fatigue crack initiation [31].

4. Conclusions

The Osprey process gives a rapidly solidified, fine grain size (typically 20 to 50 μm), homogeneous microstructure without macro-segregation, irrespective of preform thickness.

A non-particulate microstructure is generated by depositing the atomized droplets into a thin layer of semi-solid/semi-liquid metal which is maintained at the deposition surface.

Aluminium alloys can be spray-deposited without oxide films and with fine precipitates.

Spray-deposited material exhibited an average porosity level as low as 1.3%. The porosity is uniformly distributed throughout the preform.

The microstructure does not depend on the small local porosity variations revealed in this study.

The total content of oxygen of the Osprey preform (0.030 wt %) was 3.5 and 7 times lower, respectively, than the total oxygen contents of (i) the argon (nitrogen) atomized powder (0.106 to 0.110 wt %) and (ii) the air atomized powders (average value 0.209 wt %). On the basis of a heat flow analysis a cooling rate of $\sim 10^2$ to 10^4 K sec^{-1} was estimated. The silicon particle size indicated that the mean cooling rates to form 4 to 7 μm silicon precipitates are in the range 10^3 to 10^4 K sec^{-1}. This cooling rate proves that the theoretical estimation presented in this work is sufficiently accurate.

Acknowledgements

The authors are indebted to Professor Dr. Ir. B. M. Korevaar for providing facilities for this investigation and for stimulating discussions, to Mrs T. L. J. de Haan, T. Tobi and A. H. L. M. Klijnhout for skilful assistance with the experiments, and to Mr A. M. J. W. Bakker for providing the micrographs. We would like to thank Drs A. G. Leatham and A. J. W. Ogilvy for helpful discussions. The financial support of the National Polytechnic Institute in Mexico (IPN), and the Royal Academy of Science in the Netherlands (KNAW), the Foundation for Technological Research (STW) and the Foundation for Fundamental Research of Matter (FOM) is gratefully acknowledged. The preforms were supplied by Osprey Metals Ltd.

References

1. J. DUSZCZYK, J. L. ESTRADA, B. M. KOREVAAR, Z. FANG, T. L. J. DE HAAN and P. COLIJN, Technical Report for Showa Denko K. K. (Tokyo, Japan) Delft University of Technology, the Netherlands, October 1987.
2. J. L. ESTRADA, J. DUSZCZYK, B. M. KOREVAAR and R. YOSHIMURA, in Proceedings of the International Conference on Sintering 1987, edited by S. Somiya (Elsevier Applied Science, London, 1988) p. 581.
3. R. D. BRICKNELL, *Metall. Trans. A* **17A** (April 1968) 583.
4. K. OGATA, E. LAVERNIA, G. RAI and N. J. GRANT, *Int. J. of Rapid Solidification* **2** (1986) 21.
5. J. DUSZCZYK, J. L. ESTRADA, B. M. KOREVAAR, T. L. J. DE HAAN, D. BIALO, A. G. LEATHAM and A. J. W. OGILVY, in "Modern Developments in Powder Metallurgy", Vols 18–21 (MPIF Press, New Jersey, 1988) p. 441.
6. A. R. E. SINGER, *Met. Mater.* **4** (1970) 246.
7. *Idem, J. Inst. Met.* **100** (1972) 185.
8. Osprey Metals Ltd, UK Patent 147 239.
9. A. G. LEATHAM, R. G. BROOKS and M. YAMAN, in "Modern Developments in Powder Metallurgy" Vols 15–17 (MPIF Press, New Jersey, 1985) p. 157.
10. J. DUSZCZYK, J. L. ESTRADA, A. G. LEATHAM and A. J. W. OGILVY, in Proceedings of the 1987 P/M Group Meeting, Eastbourne, October 1987 (The Institute of Metals, London, 1987) p. 24/1.
11. A. G. LEATHAM and A. J. W. OGILVY, personal communication.
12. A. G. LEATHAM, A. J. W. OGILVY, P. F. CHESNEY and O. METELMANN, in "Modern Developments in Powder Metallurgy", Vols 18–21 (MPIF Press, New Jersey, 1988) p. 475.
13. J. DUSZCZYK, J. L. ESTRADA, B. M. KOREVAAR, Z. FANG, T. L. J. DE HAAN and P. COLIJN, Technical Report for the Osprey Metals Ltd (Neath, UK) Delft University of Technology, the Netherlands, April 1987.
14. D. APELIAN, B. H. KEAR and H. W. SCHADLER, in "Rapidly Solidified Crystalline Alloys", edited by S. K. Das, B. H. Kear and C. M. Adam (Met. Soc. of AIME, Warrendale, Pennsylvania, 1985) p. 93.
15. E. J. LAVERNIA, E. M. GUTIERREZ, J. SZEKELY and N. J. GRANT, *Int. J. of Rapid Solidification* **4** (1988) 89.
16. R. W. EVANS, A. G. LEATHAM and R. G. BROOKS, *Powder Metall.* **28** (1985) 13.
17. E. J. LAVERNIA, G. RAI and N. J. GRANT, *Int. J. of Powder Metall.* **22** (1986) 9.
18. A. R. E. SINGER and R. W. EVANS, *Met. Tech.* **10** (February 1983) 61.
19. J. L. ESTRADA and J. DUSZCZYK, accepted for publication in the *J. of Mater. Sci.* **25** (1990) 886.
20. A. G. LEATHAM and R. G. BROOKS, in "Modern Developments in Powder Metallurgy", Vol. 15 (MPIF Press, New Jersey, 1984) p. 157.
21. E. GUTIERREZ-MIRAVETE, E. J. LAVERNIA, G. M. TRAPAGA and J. SZEKELY, *Int. J. of Rapid Solidification* **4** (1988) 125.
22. E. GUTIERREZ-MIRAVETE, E. J. LAVERNIA, G. M. TRAPAGA, J. SZEKELY and N. J. GRANT, *Met. Trans. A* **20A** (January 1989) 71.
23. M. BECKER, in "Heat Transfer: A Modern Approach" (Plenum Press, New York, 1986) p. 131.
24. J. SZEKELY and N. J. THEMELIS, in "Rate Phenomena in Process Metallurgy" (Wiley, New York, 1971) p. 236.
25. W. J. BEEK and K. M. K. MUTZALL, in "Transport Phenomena" (Wiley, New York, 1975) p. 194.
26. D. R. PITTS and L. E. SISSOM, in "Theory and Problems of Heat Transfer" (Schaum's Outline Series, McGraw-Hill, New York, 1977) p. 316.

27. T. W. CLYNE, R. A. RICKS and P. J. GOODHEW, *Int. J. of Rapid Solidification,* **1** (1984–1985) 59.
28. W. J. BOETTINGER and S. R. CORIELL, in "Science and Technology of Undercooled Melt", edited by P. R. Sahm, H. Jones and C. M. Adam (Martinus Nijhoff Publishers, Dordrecht, 1986), p. 81.
29. J. DUSZCZYK and P. JONGENBURGER, *Powder Metall.* **29** (1986) 20.
30. J. DUSZCZYK and J. L. ESTRADA, in Proceedings of the Australian Bicentennial International Congress in Mechanical Engineering, New Materials and Processes for Mechanical Design, Brisbane, May 1988, No. 88/4 (Institute of Engineers, Australia, 1988) p. 96.
31. J. DUSZCZYK, J. L. ESTRADA, T. L. J. DE HAAN, A. G. LEATHAM and A. J. W. OGILVY, in Proceedings of the P/M Aerospace Materials Conference, Luzern, 1987 (MPR Publishing Service Ltd, Shrewsbury, UK, 1987) p. 26/1.

Received 26 April
and accepted 31 May 1989